

Forbidden lines in Herbig Ae/Be stars. The [O I](1F) 6300.31 Å and 6363.79 Å lines

II. Longslit observations of selected objects*

T. Böhm¹ and G.A. Hirth²

¹ European Southern Observatory, Karl-Schwarzschildstr. 2, D-85748 Garching, Germany (tboehm @ eso.org)

² Max-Planck-Institut für Astronomie, Königstuhl 17, D-69117 Heidelberg, Germany (hirth @ mpia-hd.mpg.de)

Received 19 December 1996 / Accepted 6 February 1997

Abstract. This paper presents first long-slit spectroscopic observations of the forbidden [O I](1F) emission line regions around selected pre-main sequence Herbig Ae/Be stars. Contrary to the lower-mass T Tauri stars, the observations show that the selected Herbig stars do not reveal neither signs of extended or positionally decentered [O I](1F) emission regions, nor signs of outflows or jets in the proximity of the stars emitting that forbidden line.

A high-velocity component in the emission profile has only been confirmed in the spectrum of the peculiar FU Ori star ZCma, in form of a profile showing an extended blue wing; this star is likely to have a disk or a companion star.

In the case of the prototype Herbig Ae star AB Aur the derived geometrical constraints on the size of the forbidden emission line region tend to rule out the presence of a significant circumstellar accretion disk.

Key words: stars: atmospheres – stars: circumstellar matter – stars: pre-main sequence – stars: emission-line

1. Introduction

The pre-main sequence Herbig Ae/Be stars are objects of intermediate masses ($2-5 M_{\odot}$) (Herbig 1960, Strom et al. 1972, Finkenzeller & Mundt 1984, Finkenzeller & Jankovicz 1984). They show all signs of intense stellar activity and strong stellar winds (Praderie et al. 1982, Catala et al 1986, Catala & Kunasz 1987). Their position in the HR diagram indicates that they are in the radiative contraction towards the main- sequence (Iben 1965, Gilliland 1986), and should in principle not possess any

Send offprint requests to: T. Böhm

* Based on observations collected with the 2.2 m telescope of the Max-Planck-Institut für Astronomie at Calar Alto, Spain

outer convective zone; therefore, if the young stellar evolutionary theory is correct, the classical magnetic dynamo mechanism could not be responsible for the observed phenomena. Finding the origin of this paradoxical activity is a major concern for young stellar evolution.

Two major interpretations should be studied in detail: the excess of non-radiative energy feeding the activity is i) provided by the energy of internal rotation or ii) by the gravitational energy of a circumstellar accretion disk. This question has already been addressed by Böhm (1993) by using various approaches based on high-resolution spectroscopy of an extended sample of Herbig Ae/Be stars. One of the major results of this study was the observation of centered and symmetric [O I](1F) forbidden emission lines in the observed sample of stars, which strongly questions the existence of significant circumstellar accretion disks around these young stars (Böhm and Catala 1994, hereafter “BC”).

In a recent work Corcoran & Ray (1997) present new results on the shape and the centroids of forbidden emission line profiles in an extensive sample of 56 Herbig stars observed at medium and low resolution. 28 of these stars possess detectable [O I](1F) 6300.31 Å emission. Excluding 4 objects having a high velocity emission component in the [O I](1F) 6300.31 Å line, as well as 5 other objects measured at low precision, the statistical centroid distribution is in good agreement with the results announced in BC.

In some cases Herbig Ae/Be stars show the presence of jets and outflows (Mundt 1993, Goodrich 1993), some exhibit asymmetric forbidden lines (Corcoran & Ray 1994 and 1997, Hamann 1994) and some show elongated polarization maps (Bastien and Ménard 1990), indicating that in these particular cases of deeply embedded objects a “native” circumstellar disk might still have survived, while the majority of Herbig stars seems to have evolved out of their parental cloud towards a “naked” state, including the dissipation of their fossil/juvenile disk. The confirmation of this idea proposed for the first time in BC would directly indicate that we are observing Herbig stars in very different phases of their young stellar evolution; new sup-

port of this idea is found in Corcoran & Ray (1997), who exhibit a link between the degree of embeddedness and the amount of forbidden line blueshift.

However, the existence or absence of circumstellar accretion disks around Herbig Ae/Be stars is still matter of strong debate: the important infrared excesses observed around these stars can also be interpreted in two different ways. In the case of the lower mass pre-main sequence T Tauri stars the IR excess is generally attributed to the presence of accretion disks (Adams et al. 1987, Kenyon & Hartmann 1987, Bertout et al. 1988). It has therefore been appealing to build similar models for the Herbig Ae/Be stars (Hillenbrand et al. 1992, Lada & Adams 1992). The second approach attributes this excess to a circumstellar gas and dust halo of more or less spherical shape (Berrilli et al. 1992, Hartmann et al. 1993, Miroshnichenko et al. 1997).

It is straightforward that the absence or existence of circumstellar accretion disks is of major importance for our understanding of the young stellar evolution in general.

Due to their very low probability of radiative transition, the forbidden emission lines can only form in extremely low-density regions, therefore far away from the central star. The strongest forbidden emission lines in Herbig Ae/Be stars are the [O I](1F) lines. There are again two major explanations possible to explain the centered and symmetric emission profile (BC) observed in the spectra of this category of stars: i) the lines are formed in the remote parts of the stellar wind; the line formation regions are determined by the geometry of the stellar wind, which is most probably of spherical symmetry. In the case of the prototype Herbig Ae star AB Aur an estimate of a characteristic radial distance of the shell-like line formation region is of some AU (Böhm 1993). The symmetrical and centered profile of a line formed at these distances makes therefore the presence of an important circumstellar accretion disk impossible, since the receding part of the wind would be hidden by the opaque disk and yield a blueshifted and asymmetric emission profile. The only possibility to reconcile the shape of the observed emission profiles with the presence of an important disk would be ii) the formation of the forbidden emission line in a very thin and extended “disk atmosphere”, following the surface of the disk. This atmosphere would just move in keplerian rotation together with the disk and would not present any significant orthogonal outflow velocity. This idea first proposed by Hirth et al. 1994a is based on the model of Kwan & Tademaru (1988), built for explaining the forbidden emission line profiles of the lower-mass T Tauri stars: this model contains two components, one at high velocity formed in a jet, and one “disk-atmosphere” component at almost zero radial velocity. If now, for some reason, the high-velocity component could not form, perhaps due to the different radiation field emanating from the hotter Herbig stars, the resulting profile would only be due to the low-velocity component and therefore be of symmetrical and centered appearance. However, since the emission volume of the forbidden lines has to be important due to the very low critical density of formation and the orthogonal extension of the “disk-atmosphere” can only be strongly limited, this would yield very high radial extensions of

the emission region following the disk surface, most probably of the order of 100 and more AU (Böhm 1993).

All the above considerations about the shape and extent of the forbidden emission line regions around Herbig Ae/Be stars will have to be explained, in a subsequent step, by a complete physical model, explaining also the origin and the mechanism of the heating of these emission regions. At this step, only qualitative explanations can be advanced. In the case of a forbidden emission line formed in the outermost regions of the stellar wind the emission could occur in a post-shock region. This shock would then take place at a distance where the wind encounters the circumstellar gas and dust. The energy provided by the high velocity wind is largely sufficient to heat this region. In the case of a formation in a disk-atmosphere the limited gravitational energy of the accretion disk would have to satisfy the required energy balance.

In order to elucidate this interesting question, we therefore decided to select Herbig stars corresponding to different presumed evolutionary stages, and to perform on them long-slit spectroscopy in order to get first information about the spatial properties, i.e., about the shape and extend of the associated [O I](1F) forbidden emission line regions.

Sect. 2 presents the observations and data analysis. Results are presented in Sect. 3 and discussed in Sect. 4. Finally, the conclusions are drawn in Sect. 5.

2. Observations and data reduction

Six Herbig Ae/Be stars have been selected, some of which are deeply embedded (BD +40°4124), while others show relatively low visual extinction (AB Aur, HD 250550), two of the objects show signs of collimated outflows at large distances from the star (Z CMa, BD +46°3471), while Z CMa light exhibit strong linear polarization (Vrba 1975, Jain et al. 1990). The list of the observed stars and some of the properties of their circumstellar environment are given in Table 1.

Most stars of the sample are rather distant; only AB Aur (Taurus-Auriga cloud) was close enough to expect strongly constraining results on the radial size of the forbidden emission line regions.

For these stars, we obtained long-slit spectra with the coude spectrograph of the 2.2 m telescope on the Calar Alto Observatory (Spain) of the [O I](1F) 6300.31 Å and the 6363.79 Å lines, the latter one being too weak to be included into the hereby presented analysis. The log of the observations is shown in Table 2.

We used the *f/3* camera equipped with a Ford 3 CCD chip having a pixel size of 13 μm. In spatial direction the scale results in 0.41"/pixel. The spatial resolution of the long-slit spectra was limited by the rather poor seeing, which varied between 1.5" and 2.7". The seeing was measured by the spatial width of the stellar continuum free from forbidden emission lines (Full width at half maximum $FWHM_c$, hereafter f_c). This measurement includes guiding errors and instrumental resolution. The origin of the slit positions were chosen arbitrarily, but we tried to cover most of the projected sky uniformly by increasing the position angle of the slit by 30 degrees from one spectrum to the next. Only in

Table 1. Observed stars. Columns: (1) Star. (2) Position α (2000) and (3) δ (2000). (4) Spectral types, ranges found in the literature. (5) Distances from [1] Cantó et al. (1984), [2] Claria (1974), [3] Elias (1978a), [4] Elias (1978b), [5] Herbig (1960) and [6] Cohen (1973). (6) Visual extinction (Hillenbrand et al. 1992). (7) Projected length of outflow/jet, if known ([1] Poetzel et al. 1989, [2] Goodrich 1993).

Star	α (2000) [hr min sec]	δ (2000) [deg min sec]	Spec.Type	D [pc]	A_V [mag]	jet? [arc"]
(1)	(2)	(3)		(4)	(5)	(6)
BD +40°4124	20 20 28	41 21 53	A2-B2	2000 [1]	3.0	
Z CMa	07 03 43	-11 33 06	B	1150 [2]		> 280 [1]
BD +46°3471	21 52 34	47 13 43	A0-A6	900 [3]	1.0	74 [2]
AB Aur	04 55 46	30 33 05	A0	140±20 [4]	0.4	
HD 259431	06 33 05	10 19 20	B2	800 [5]	1.6	
HD 250550	06 02 00	16 30 57	B7-A2	280 [1]	0.5	

the case of Z CMa we oriented the 73° position approximately parallel to the large scale jet (Poetzel et al. 1989). The reciprocal linear dispersion was 9 \AA mm^{-1} and the slit width $1.7''$ resulting in a spectral resolution of 23 km s^{-1} around the [OI] λ 6300 line ($R \simeq 13000$).

Data reduction was performed with the help of the “long-slit” environment of MIDAS. After the subtraction of the bias value and the subtraction of an interpolated (and cosmic-cleaned) sky-background, the spectrum was wavelength-calibrated and then rebinned in both dimensions. An optimal extraction routine yielded a 1D spectrum; a spline-fit of this continuum was then grown in the spatial direction and normalized to unity at the rest-wavelength of the [OI](1F) 6300 \AA line. The 2D long-slit spectrum was hereafter divided by this artificial image. As a result we obtained a cleaned, wavelength-calibrated long-slit spectrum with a flat continuum, including yet all the flux information. In order to extract the information contained in the relatively weak emission line profiles, we performed a subtraction of the stellar continuum. In order to regenerate an artificial continuum at the position of the line, columns left- and rightwards of the emission line have been interpolated and extended in the spectral direction to a 2D pseudo-continuum image. The correct reconstruction of this artificial continuum is extremely crucial; the dominant errors leading to the upper limits of the measured final results (spatial centroid and extend of the forbidden emission line regions) depend strongly on this procedure; telluric water lines do not facilitate this task. Finally the 2D spectra were put in the barycentric velocity reference frame and the wavelength scale translated in velocities. In the spatial direction pixels have been translated in arcseconds of displacement with respect to the position of the continuum.

3. Results

3.1. Spectral properties

The spectral properties of the [OI] λ 6300 line of the Herbig Ae/Be stars are listed in Table 3. It should be noticed that the measured equivalent width (EW) do not differ significantly from the values announced in paper BC, except in the case of BD+40° 4124, where the EW seems to have dropped by about

25% within the 13 years between the two observations. Significant profile changes have not been detected; slightly lower FWHM-values in this paper might be due to the very different resolving power of the instruments used; values in this paper have been corrected for the comparatively large resolved element by quadratic subtraction of the width of the instrumental profile.

The radial velocities of the line centroids correspond well to the stellar velocities and the velocities of the associated molecular clouds.

In the case of Z CMa the [OI] λ 6300 line extends up to at least -230 km s^{-1} in the blue. This emission obviously represents the high velocity blueshifted part of the outflow (cf. Edwards et al. 1987, Poetzel et al. 1989).

3.2. Spatial properties

The most interesting results of these long-slit spectroscopic observations of selected Herbig Ae/Be stars is the fact that none of the objects shows a spatially extended FEL in [OI] λ 6300, and this in none of the different investigated positional angles. However, our results are strongly limited by the following factors, listed by decreasing order of significance: i) the quality of the seeing, ii) the precise determination of a pseudo-continuum under the line (which is difficult in a region full of telluric lines), iii) the S/N of the spectra and iv) the contrast of the emission lines with respect to the continuum; in fact, a lower contrast of the line gives point ii) a higher importance. Other parameters might play a role, but the dominant ones are listed above. A further error factor enters when converting the upper limits of the derived FWHM of the forbidden emission line regions from angular scales into projected distances, due to the uncertainties of the distances taken from the literature. As a matter of comparison, we indicate in appendix A the theoretical uncertainties under the major hypothesis of the perfect subtraction of a flat continuum (in spectral *and* in spatial sense) and a gaussian spatial emission profile. Despite their academic value, these results show that typical uncertainties due to photon noise are much lower than the uncertainties we determined from our measurements.

Table 2. Log of the long-slit spectroscopic observations at the Calar Alto 2.2 m telescope.

Star	Date	UT _{mid}	t _{exp}	PA	Seeing
(1)	[ddmmyy]	[hrs]	[s]	[deg]	[arc"]
	(2)	(3)	(4)	(5)	(6)
BD+40°4124	11 11 94	19:03	1500	90	1.47
	"	19:47	2000	120	1.86
	"	20:35	"	150	1.73
	"	21:22	2500	180	1.82
	"	22:25	"	210	1.77
ZCMa	12 11 94	04:08	2000	0	2.42
	"	05:23	2167	73	2.40
BD+46°3471	14 11 94	18:28	2800	90	1.48
AB AUR	14 11 94	20:50	2500	90	1.66
	"	21:42	"	240	2.08
	"	22:27	"	210	1.96
	"	23:20	"	180	1.88
	"	00:04	"	150	1.89
	15 11 94	00:48	"	120	1.91
HD 259431	14 11 94	00:18	3000	0	2.61
	"	01:15	"	30	2.70
	"	02:21	"	60	2.48
	"	03:15	"	90	2.15
	"	04:07	"	120	2.11
"	05:00	"	150	2.13	
HD 250550	15 11 94	01:47	2500	90	1.99
	"	02:36	"	120	2.06
	"	03:19	"	150	2.31
	"	04:03	"	180	2.21
	"	04:46	"	210	2.07
"	05:26	1930	240	2.07	

The combination of the errors described above were statistically estimated on all positional angles from the different stars, using results derived from two different estimators: i) the averaged spatial offset and enlargement of the total line profile collapsed in the spectral sense (for all columns supporting the emission line) and ii) the same values, but only on the maximum intensity column (corresponding in general to the line centroid). Errors made in the generation of the pseudo-continuum are included in the estimation.

After subtracting the interpolated continuum from the spectrum, we measured on all residual emission line profiles their centroids and their *FWHM*, and this for the two estimators cited above. However, the number of estimations could vary between 1 and 3 per positional angle. We then decided to identify the 0° direction with an arbitrary *x*-axis and the 90° direction with its corresponding perpendicular *y*-axis. Each centroid measurement was then projected on both axes according to the corresponding slit angle of the given spectrum. A statistical study

Table 3. Spectral properties of the [OI]λ 6300 line of the observed stars. Columns: (1) Star. (2) Heliocentric radial velocity. ZCMa shows an extended red absorption and blue emission wing and a highly asymmetric spectral profile; therefore, no *v_{hel}* value has been listed in this table. (3) Radial velocity of the associated molecular cloud / the star / and the Ca II interstellar line (summarized in Finkenzeller & Jankovics 1984). (4) Velocity dispersion corrected for the instrumental profile. (5) Equivalent width.

Star	<i>v_{hel}</i>	<i>v_{MC/v_*}</i> / <i>v_{CaII}</i>	Δ <i>v_{hel}</i>	W _λ
(1)	[km s ⁻¹]	[km s ⁻¹]	[km s ⁻¹]	[Å]
BD +40°4124	-3	-9/-8±6/-	54	-1.12
ZCMa	-?	+32/-/-	-?	
HD 259431	+28	+20/+43±20/+19±4	35	-0.50
BD +46°3471	-	-7/-/-14±4	-	W _λ < 0.05
AB Aur	+18	+16/+21±10/+19±4	26	-0.12
HD 250550	+15	+16/+31±26/+16±4	23	-0.09

was then performed on both samples of *x*- and *y*-values, yielding mean-values, standard errors (*σ*) and standard errors of the mean (*σ_m*) for the displacements in both directions. The physical significance of these results depends on the hypothetical shape and extension of the forbidden emission line region. Since the spectral profile of the observed forbidden emission lines is (except in the case of ZCMa) highly symmetric, the assumption that the forbidden emission line region (FELR) extends over *all* slit positions is rather conservative. In this case, the probability that the centroid of the FELR is situated within a distance of 2 *σ_m* from the mean value is about 95%. However, if the assumption cited above does not apply and the FELR is produced in a highly collimated jet very close to the star (which is not likely due to the big required emission volume), then the standard deviation of a given measurement (*σ*) would be a better estimation of the precision.

The full width of half maximum of all least-square fitted measurements were treated like scalar data (and not projected following the positional angles). After having precisely determined the *FWHM* (*f* in the following) of the continuum (*f_c*) and of the emission line (*f_i*), we calculated the difference between both, Δ*f* = *f_i* - *f_c*. Since the uncertainty on the value of *f* increases significantly with its size (and therefore with the seeing), we decided to calculate the “fractional difference” *k* = Δ*f*/*f_c*. We obtained a similar amount of positive and negative values, which clearly shows that Δ*f* measures error bars of the continuum subtraction method and not realistic contributions of the spatial extent of the FELR. Nevertheless, in order to determine an upper limit of the *f*-size of the FELR in accordance with our observations, we calculated the mean value of the “fractional difference” < *k* >, its standard deviation *σ*(*k*) and the standard deviation of the mean, *σ_m*(*k*). Again, under the conservative assumption of a circularly shaped and uniformly extended FELR, the standard deviation of the mean (for all different positional angles of a given star) yields a good estimate

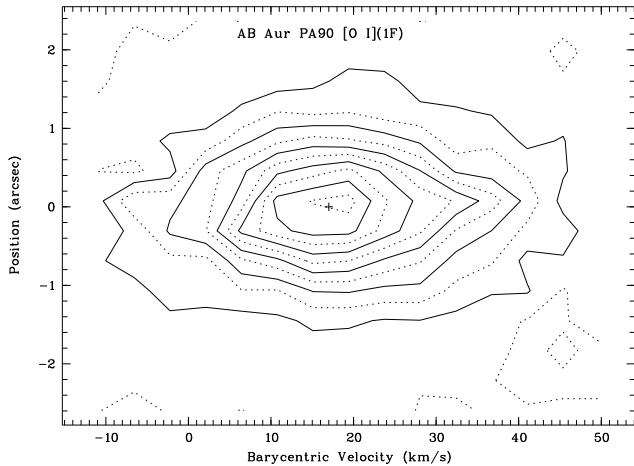


Fig. 1. Position-velocity diagram of the [O I] λ 6300 line of AB Aur at PA 90°. The cross indicates the radial velocity of the associated molecular cloud (see Table 3), which corresponds well to the maximum of the emission peak. All velocities are in the barycentric frame. Note that no spatial extension exceeding the width of the continuum and no high velocity component can be discerned.

of the upper limit of the extension; if the uncertainty on a single measurement is looked for (which would be important for a jet-like structure), the interesting value would be $\sigma(k)$. Individual measurements differing more than 3 times the standard deviation from the mean are not present.

Taking these statistical results into account, we can therefore derive from the position-velocity diagrams upper limits of the corrected spatial full width at half maximum f_{FEL} and the offset of the centroid position y_{FEL} of the forbidden emission line region relative to the stellar position. Taking $f_l = f_c + \Delta_f$ and assuming a gaussian profile of the FELR we can write:

$$(f_c + \Delta_f)^2 = f_c^2 + f_{FEL}^2$$

and derive the inequality:

$$\sqrt{2\sigma(k)} f_c \geq f_{FEL}$$

(the mean values of k are not significant and dominated by the standard deviation).

Table 4 summarizes the spatial properties of the observed long-slit spectra as well as upper limits of the centroid displacements and the extensions of the forbidden emission line regions under the two extreme uncertainties, i.e. σ and σ_m , reasonable estimates are most probably in between.

Fig. 1 shows the velocity-position diagram for AB Aur at PA 90°. Note that no spatial extension exceeding the width of the continuum and no high velocity component can be discerned.

Note that also for ZCma we have not been able to find a spatial offset of the emission centroid of the [O I] λ 6300 line in the direction of the jet (cf. Poetzel et al. 1989); due to its asymmetric and noisy profile we did not include the spectra of this star in Table 4. Fig. 2 show the velocity-position diagram

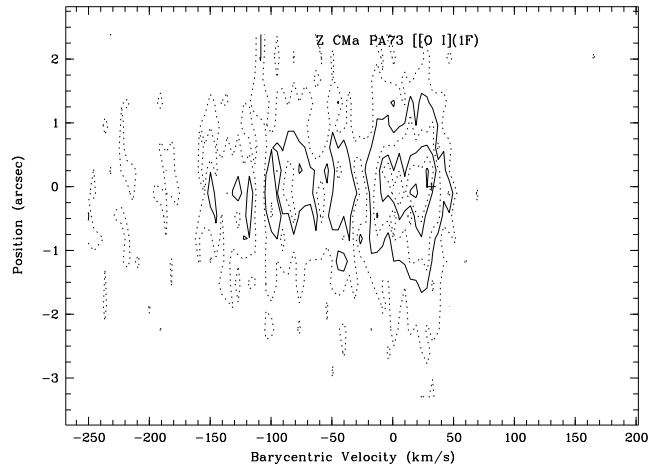


Fig. 2. Position-velocity diagram of the [O I] λ 6300 line of ZCma PA 73°. The cross indicates the radial velocity of the associated molecular cloud (see Table 3), which corresponds well to the maximum of the emission peak. All velocities are in the barycentric frame. No spatial shift of the centroid can be detected, not even for the highly blueshifted parts of the line.

for ZCma at PA 73°. BD +46°3471 also does not reveal any apparent extension of the [O I]-FELR, although the emission was too weak and too noisy to draw significant conclusions.

4. Discussion

The results obtained by this study are untypical compared to observations of TTSS, which in most cases display an offset of the emission centroid in the FELRs (Hirth & Mundt 1996, Hirth et al. 1994a, 1994b), frequently even of several arcseconds. For example, V 536 Aql displays such an offset in the low- and high velocity component. In this study, none of the individual measurements of the positional offsets for all the observed stars presented in Table 4 and all positional angles showed any significant offset, and the corresponding measurement uncertainties did in no case exceed 0.2 arcseconds.

This supports the idea that the circumstellar environment of Herbig Ae/Be stars are very different compared to their lower mass counterparts, the T Tauri stars. High velocity components of the forbidden lines are supposed to form in bipolar outflows, which are basically driven by the magnetic field from a circumstellar accretion disk (Kwan & Tademaru 1988, 1995). The absence of this high velocity component in Herbig stars could indicate therefore directly the absence of important circumstellar accretion disks, unless the formation of this component is compromised due to other reasons, e.g. due to the ionization by the higher temperature continuum radiation field of the Herbig stars (Hirth et al. 1994a, Hirth 1994).

However, the fact that the forbidden emission line regions from the stars listed in Table 4 are well centered in the spatial and in the spectral direction shows that there must be a high degree of symmetry in these regions: the observed lines can not

Table 4. Spatial properties of the long-slit spectra and inferred upper limits on the forbidden emission line regions and their centroids. Columns: (1) Star. Top: Upper limits for the centroid displacement(in arc''): (2) $\langle x \rangle$, (3) $\sigma(x)$ and (4) $\sigma_m(x)$, (5) $\langle y \rangle$, (6) $\sigma(y)$ and (7) $\sigma_m(y)$. (8) Fractional difference $\langle k \rangle$, (9) $\sigma(k)$ and (10) $\sigma_m(k)$ in percentage of seeing. Bottom: (2)-(7) id. top, but in AU. (8), (9) and (10) upper limits in AU of the $FWHM$ of the FELR derived from our observations, calculated by $f_{FEL} \leq \sqrt{2} \langle k \rangle f_c$, $f_{FEL} \leq \sqrt{2} \sigma(k) f_c$ and $f_{FEL} \leq \sqrt{2} \sigma_m(k) f_c$ (Note that the estimations based on the mean value is situated between the results calculated with the different standard deviations (cols. 9 and 10); however, since the mean value has in some cases a negativ sign, physically more meaningful results come from the latter estimators given in cols. 9 and 10). “nc”: not calculated, negative square-root makes no sense in that context.

(1) Star	(2) $\langle x \rangle$ [arc'']	(3) $\sigma(x)$ [arc'']	(4) $\sigma_m(x)$ [arc'']	(5) $\langle y \rangle$ [arc'']	(6) $\sigma(y)$ [arc'']	(7) $\sigma_m(y)$ [arc'']	(8) $\langle k \rangle$ [% seeing]	(9) $\sigma(k)$ [% seeing]	(10) $\sigma_m(k)$ [% seeing]
BD +40°4124	0.000	0.018	0.006	-0.021	0.037	0.012	-1.1	8.2	1.0
AB Aur	0.012	0.036	0.010	0.024	0.048	0.013	1.9	7.7	0.6
HD 259431	-0.017	0.026	0.007	-0.011	0.018	0.005	1.4	3.3	0.3
HD 250550	0.025	0.105	0.035	0.003	0.082	0.027	-7.9	14.1	1.57
	[AU]	[AU]	[AU]	[AU]	[AU]	[AU]	[AU]	[AU]	[AU]
BD +40°4124	0	36	13	-41	67	24	nc	1411	499
AB Aur	1.7	5.0	1.4	3.4	6.7	1.8	52	104	29
HD 259431	-13	21	6	-8	14	4	322	487	147
HD 250550	7	29	10	1	23	8	nc	317	106

form in the blueshifted and spatially decentered parts of a bipolar outflow, whose receding lobe is hidden by a circumstellar disk.

Nevertheless, in some exceptional cases blueshifted FELs have been reported in spectra of particular Herbig stars (Edwards et al. 1987, Corcoran & Ray 1994, Hamann 1994, BC), which also show different other signs of the presence of circumstellar disks; in these cases a clear analogy to Classical T Tauri stars can be seen.

Unfortunately the derived upper limits of the $FWHM$ of the FELR suffer from the bad seeing during the observations, since they are directly proportional to it. Moreover, the rather high distances to most of the selected stars (typically 800 to 1000 pc) and the large uncertainties on the determination of the distances of the remote objects do not allow the derivation of strong constraints from our observations.

Only in the case of AB Aur a really constraining upper limit of the FELR- $FWHM$ could be derived. The $1-\sigma$ limit of the $FWHM$ is 104 AU for a single long-slit spectrum, but, assuming a uniformly extended emission region affecting all the position angles, the upper limit is only 29 AU. At this place we want to reinspect on the fact that all derived $FWHM$ sizes are just upper limits due to the uncertainties of the methods and the measurements, they are not real detections. Hillenbrand et al. (1992) modeled the strong IR-excesses observed in the spectra of these stars by circumstellar accretion disk emission and obtained inner and outer disk radii. In the case of AB Aur the inner disk radius should be very small ($7 R_*$), while the outer radius has to be bigger than 29 AU. Thus, the hypothetical disk would cover most of the FELR and the only way to reconcile the spectral and spatial symmetry of the line with the presence of a disk would be to form it in a disk-atmosphere broadened by keplerian rotation. Taking into account the very high emission

volume and given the constraint on the $FWHM$ derived in this article, it seems impossible that the [O I](1F) lines form in such a thin disk-atmosphere (Böhm 1993).

Quantitative modelling has still to confirm the conclusion of these geometrical investigations. Moreover, higher quality determinations of the distances of our objects should be carried out in order to reduce the corresponding errors.

For the other observed stars our results are not constraining enough to eliminate the hypothesis of the presence of a disk around these stars. However, the obtained results are still constraining the sizes and the centroids of the forbidden emission line regions of the [O I](1F) lines. In the case of Z CMa and BD +46°3471 no deep statistical analysis could be performed due to the low quality of the obtained spectra, but both stars do not exhibit any apparent positional offset nor any extension of the [O I]-FELR in their long-slit spectra.

5. Conclusions

Despite the poor seeing conditions, the analysis of long-slit spectra of some selected Herbig Ae/Be stars show major differences compared to the lower-mass T Tauri stars. Within the uncertainties of the measurement (and the associated methodological errors) and considering the large distances to most of the objects, no extended forbidden [O I](1F) emission line region could be detected. Except in the case of Z CMa, no spectrum of the observed stars shows any sign of a high-velocity component (unlike in the case of the T Tauri stars).

In the case of AB Aur, the prototype Herbig Ae star in the northern hemisphere, the geometrical constraints on the size of the FELR of the [O I](1F) lines seem to rule out the existence of an important, optically thick, circumstellar accretion disk. This

Table 5. Theoretical uncertainties on the determination of the $FWHM$ and the centroid of the forbidden emission lines by least square fit to a gaussian profile built by photons. Examples calculated for different stars of the sample following appendix A. Columns: (1) Star and position angle. (2) Maximum signal in ADU of the continuum and the line. (3) $FWHM$ of the continuum in spatial direction and $FWHM$ of the line in spectral direction (uncorrected for resolution, in pixel). (4) Uncertainty on the spatial centroid of the continuum (left) and uncertainty on the spatial centroid of the line with respect to the continuum (quadratic addition of the uncertainties), (right). The spatial centroid uncertainties are translated in angular uncertainties (arcseconds). (5) Uncertainty on the spatial $FWHM$ of the continuum (left) and the line (right), expressed in percentage of the seeing.

Star,(PA)	ADU max. (Cont., Line)	$FWHM$ (pixel) (Spatial, Spectral)	Δ_{y0} (arc") (Cont., Line)	Δ_f (%seeing) (Cont., Line)
(1)	(2)	(3)	(4)	(5)
BD +40°4124 (150)	143, 121	4.23, 12	0.017, 0.019	2, 1.2
AB Aur (90)	3560, 520	4.1, 7	0.003, 0.012	0.4, 1.4
HD 259431 (120)	616, 337	5.15, 8	0.009, 0.014	0.9, 1
HD 250550 (90)	288, 50	4.85, 6.5	0.013, 0.042	1.3, 4

result tends therefore to confirm previous investigations on this star (Böhm & Catala 1993, BC).

Further models have to take into account the upper limits derived for the forbidden [O I](1F) emission line regions around these stars. A more precise determination of the distances of the observed objects would be of great help.

Spectro-imaging observations with adaptive optics would be the next step to bring light in the investigations of these interesting objects.

Acknowledgements. We would like to thank Prof. J. Landstreet, Drs. C. Catala and J.-F. Donati for many fruitful discussions. We are indebted to the Calar Alto staff for assistance during the observing run.

Appendix A: precision of LQ-fits to gaussian profiles

In Yoshizawa et al. (1985) we can find the generalized solution of the precision of a least square fit to a given photonic profile, taking into account the poisson noise of the distribution. In the case of a simple gaussian profile of maximum flux I_{max} , total intensity I and full width at half maximum f the uncertainty on the determination of the full width Δ_f and on the centroid Δ_{y0} find the simple expressions, in the case of a large amount of photons I :

$$\Delta_{y0} \simeq \frac{f}{2\sqrt{I}} \quad (\text{A1})$$

$$\text{and} \quad \Delta_f \simeq \frac{f}{\sqrt{I}} \quad (\text{A2})$$

These results translate the fact that the uncertainties scale with the spatial width of the profile, but vary inversely to the square root of the total flux under the profile, i.e. the integrated signal to noise value.

Supposing now that an emission line of integrated intensity I_l is rising on top of the continuum of intensity I_c . After a hypothetically perfect subtraction of the continuum the residual

profile will be the one of the line, of integrated flux I_l , but the noise of the profile will be determined by the noise due to the photons of the line *and* the photons of the continuum. Therefore, the precision of the least square fit to the residual profile should now be expressed as the following:

$$\Delta_{y0} \simeq \frac{f\sqrt{I_l + I_c}}{2I_l} \quad (\text{A3})$$

$$\text{and} \quad \Delta_f \simeq \frac{f\sqrt{I_l + I_c}}{I_l} \quad (\text{A4})$$

If several columns m in the spatial direction are averaged before the fitting, the total flux to be used is obviously $m \times I$, i.e. the flux of a single column multiplied by the number of columns.

As an example, let us estimate the different uncertainties of the least square fit in the case of the long-slit spectrum of AB Aur. The continuum right- and leftwards of the line peaks at 3560 ADU (analog/digital units), while the line exceeds the continuum of about 520 ADU. In spectral direction the $FWHM$ of the line is close to 7 pixels (uncorrected for the instrumental resolution), in spatial direction 4.1 pixels. The CCDs conversion factor is close to 2 electrons/ADU. We average one column of continuum left- and one rightwards the emission line and then expand the result in the spectral direction before subtracting it finally from the total spectrum. For the precisions of the continuum fit equations A1 and A2 apply, with I multiplied by 2 ($m=2$ here). The obtained uncertainties are therefore: $\Delta_{y0} \simeq 4.1/(2\sqrt{2} \times 3560 \times 4.1 \times 2) \simeq 0.008$ pix, and $\Delta_f \simeq 0.017$ pix. These theoretical results are based on the rough hypothesis that the spatial profile is a perfect gaussian. The line profile is collapsed in the spectral direction before performing a LQ fit. The total flux in the line is therefore $I_l \simeq 520 \times 4.1 \times 7 \times 2 \simeq 29848$ photoelectrons. The flux in the continuum relevant for the noise determination is the flux in one column divided by the square root of the number of averaged columns ($m=2$ here), multiplied by the spectral FWHM

in pixel of the line: $I_c \simeq 144494$ photoelectrons. Therefore: $\Delta_{y0} \simeq 0.03$ pix, $\Delta_f \simeq 0.06$ pix. These pixel uncertainties are translated in angular uncertainties by the multiplication with $0.41''/\text{pix}$. Results for the other stars are listed in Table 5.

We see that all these uncertainties are dominated by the measured errors indicated in cols. 3, 6 and 9 of Table 4, most probably due to the unprecise continuum subtraction, the presence of telluric lines, etc.

References

- Adams, F.C., Lada, C.J., Shu, F.H., 1987, ApJ, 312, 788
 Bastien, P., Ménard, F., 1990, ApJ, 364, 232
 Berrilli, F., Corciulo, G., Inghrosso, G., Lorenzetti, D., Nisini, B., Strafella, F., 1992, ApJ, 398, 254
 Bertout, C., Basri, G., Bouvier, J., 1988, ApJ, 330, 350
 Böhm, T., 1993, *Thèse de Doctorat*, Université Paris 7
 Böhm, T., Catala, C., 1993, A&AS, 101, 629
 Böhm, T., Catala, C., 1994, A&A, 290, 167 (paper BC)
 Cantó, J., Rodríguez, L.F., Calvet, N., Levreault, R.M., 1984, ApJ, 282, 631
 Catala, C., Czarny, J., Felenbok, P., Praderie, F., 1986, A&A, 154, 103
 Catala, C., Kunasz, P.B., 1987, A&A, 174, 158
 Claria, J.J., 1974, AJ, 79, 1022
 Cohen, M., 1973, MNRAS, 164, 395
 Corcoran, M., Ray, T.P., 1994, in “First Conf. on the Nature and Evol. Status of Herbig Ae/Be stars”, eds. P.S. Thé, M.R. Pérez and E.P.J. v.d. Heuvel, Amsterdam (1993), A.S.P. Conf. Ser., Vol. 62, 151
 Corcoran, M., Ray, T.P., 1997, A&A, in press
 Edwards, S., Cabrit, S., Strom, S.E., Heyer, I., Strom, K.M., Anderson, E., 1987, ApJ, 321, 473
 Elias, J.H., 1978a, ApJ, 223, 859
 Elias, J.H., 1978b, ApJ, 224, 857
 Finkenzeller, U., Mundt, R., 1984, A&AS, 55, 109
 Finkenzeller, U., Jankovics, I., 1984, A&AS, 57, 285
 Gilliland, R.L. 1986, ApJ, 300, 339
 Goodrich, R., 1993, ApJS, 86, 499
 Hamann, F., 1994, ApJS, 93, 485
 Hartmann, L., Kenyon, S.J., Calvet, N., 1993, ApJ, 407, 219
 Herbig, G.H., 1960, ApJS, 4, 337
 Hillenbrand, L.A., Strom, S.E., Vrba, F.J. Keene, J., 1992, ApJ, 397, 613
 Hirth, G.A., 1994, in “First Conf. on the Nature and Evol. Status of Herbig Ae/Be stars”, eds. P.S. Thé, M.R. Pérez and E.P.J. v.d. Heuvel, Amsterdam (1993), A.S.P. Conf. Ser., Vol. 62, 270
 Hirth, G.A., Mundt, R., Solf, J., 1994a, A&A, 285, 929
 Hirth, G.A., Mundt, R., Solf, J., 1994b, ApJ, 427, L99
 Hirth, G.A. Mundt, R. 1996, A&A, submitted
 Iben, I., Jr. 1965, ApJ, 141, 993
 Jain, S.K., Bhatt, H.C., Sagar, R., 1990, A&AS, 83, 237
 Kenyon, S.J., Hartmann, L. 1987, ApJ, 323, 714
 Kwan, J., Tadamaru, E., 1988, ApJ, 332, L41
 Kwan, J., Tadamaru, E., 1995, ApJ, 454, 382
 Lada, C.J., Adams, F.C., 1992, ApJ, 393, 278
 Miroshnichenko, A., Ivezić, Z., Elitzur, M., 1997, ApJ Letters, in press
 Mundt, R., 1993, in “Stellar Jets and Bip. Outflows”, eds. L. Errico, A. Vittone (Kluwer, Dordrecht), p.91
 Poetzel, R., Mundt, R., Ray, T.P., 1989, A&A, 224, L13
 Praderie, F., Talavera, A., Felenbok, P., Czarny, J., Boesgaard, A.M., 1982, ApJ, 254, 658
 Strom, S.E., Strom, K.M., Yost, J., Carrasco, L., Grasdalen, G., 1972, ApJ, 173, 353
 Vrba, F., 1975, ApJ, 195, 101
 Yoshizawa, M., Andreassen, E., Hog, E., A&A, 147, 227